processes

MDPI

Article

An Experimental Study on the Flash Boiling Characteristics of Liquid Ammonia Spray in a Constant Volume Chamber under High Injection Pressure

Haibin He [1], Jie Wu [1], Lei Wang [1], Hua Lou [1], Songfeng Li [1], Lvmeng Huang [2] and Zhanming Chen [1,2,*]

[1] Ningbo C.S.I. Power & Machinery Group Co., Ltd., Ningbo 315020, China; hehaibin@ningdong.com (H.H.); wujie@ningdong.com (J.W.); wanglei@ningdong.com (L.W.); louhua@ningdong.com (H.L.); lisongfeng@just.edu.cn (S.L.)

[2] Shaanxi Key Laboratory of New Transportation Energy and Automotive Energy Saving, Chang'an University, Xi'an 710064, China; hlm456417@163.com

* Correspondence: zm_chen@chd.edu.cn

Abstract: The spray characteristics of liquid ammonia under various ambient pressures and temperatures were analyzed in a constant volume chamber to cover a wide range of superheat degrees. The injection pressure was set as 70 and 80 MPa with ambient pressure ranging from 0.2 to 4 MPa. The ambient temperature was 500 K. The results showed that the higher the injection pressure, the greater the kinetic energy obtained. The droplet fragmentation was enhanced, and the phenomenon of gradual separation of the gas–liquid region occurred with increasing injection pressure. Under flash boiling spray conditions, the spray developed faster than non-flash boiling and transition flash boiling spray under the same injection pressure. In addition, the flash boiling spray tip penetration of the gas and liquid increased more than that of cold spray, and the fluctuation of the late stage of the injection was relatively large. Therefore, the injection pressure has a greater effect on the spray tip penetration of flash boiling spray. Moreover, ambient pressure greatly influences the flare flash boiling spray. The spray resistance phenomenon was found during the spray development in the flare flash boiling condition. With the increase in ambient pressure, the spray tip penetration of flash boiling spray decreases due to the reduction in the pressure difference inside and outside the spray hole and the restriction of ambient gas. Meanwhile, owing to the low ambient pressure and ambient density, the liquid penetration in the initial phase of the flare flash boiling spray will be abnormally shorter than that of the non-flash boiling spray.

Keywords: ammonia; flash boiling spray; high pressure injection; optical study

check for updates

Citation: He, H.; Wu, J.; Wang, L.; Lou, H.; Li, S.; Huang, L.; Chen, Z. An Experimental Study on the Flash Boiling Characteristics of Liquid Ammonia Spray in a Constant Volume Chamber under High Injection Pressure. *Processes* **2024**, *12*, 1076. https://doi.org/10.3390/pr12061076

Academic Editors: Tiemin Xuan, Hongliang Luo, Chang Zhai and Pengbo Dong

Received: 17 April 2024
Revised: 18 May 2024
Accepted: 22 May 2024
Published: 24 May 2024

Copyright: © 2024 by the authors. Licensee MDPI, Basel, Switzerland. This article is an open access article distributed under the terms and conditions of the Creative Commons Attribution (CC BY) license (https://creativecommons.org/licenses/by/4.0/).

1. Introduction

Owing to the urgent requirement of global economy decarbonization, the internal combustion engine can achieve zero carbon emissions by utilizing carbon-free and carbon-neutral fuels and sustainably leveraging its advantages of high efficiency, energy density, and reliability [1]. Ammonia, as a type of carbon-free fuel, released only nitrogen and water emissions when it completely burned. As a renewable fuel, ammonia can be synthesized from hydrogen, which can be widely produced from renewable energies, such as wind, solar, and tidal energy [2]. As a vital hydrogen carrier, ammonia has superior properties in fuel storage, transportation, and large-scale production. In addition, the volumetric energy density of liquid ammonia is 1.6 times larger than that of liquid hydrogen. Furthermore, ammonia is safer than hydrogen in transportation and storage; thus, it can be easily detected when leaking occurs. Therefore, ammonia is regarded as the most promising alternative fuel for internal combustion engines [3].

However, there are some challenges when using ammonia in internal combustion engines related to the poor combustion characteristics of ammonia [4]. First, the low heating

value (LHV) of ammonia is 18.5 MJ/kg, which is considerably lower than that of diesel (LHV = 43.5 MJ/kg) and natural gas (LHV ≈ 47.2 MJ/kg) [5]. Second, the laminar flame speed of ammonia is less than 9 cm/s, which is much lower than that of hydrocarbon fuel under the same conditions [6]. Third, the flammability of ammonia is much lower than other traditional fuels. Therefore, these approaches, such as hydrogen assistance, dissociation prior to combustion, and blending with other fuels with good autoignition properties, must be taken into consideration to overcome the barrier for ammonia utilization on internal combustion engines [7].

Consequently, fuel combustion mode—a secondary fuel with good combustion properties—was used to improve the poor combustion intensity of ammonia. Liu et al. optimized combustion and reduced ammonia emission by introducing hydrogen into the precombustion chamber to generate a dispersed jet reaction [8]. However, the traditional dual fuel engine with ammonia port injection still suffered from problems such as low ammonia substitution ratio, high unburned emission, and great NOx emissions [9]. Changing the injection strategy of ammonia from port injection to direct injection can effectively increase the ammonia substitution ratio and control the unburned emission. This is because ammonia direct injection with high pressure is preferred to provide sufficient ammonia fuel and precisely controls the air-fuel ratio [5]. In addition, the mixture formation, combustion regulation, and emission reduction can be easily controlled in the diffusive combustion mode when ammonia direct injection is adopted. Thus, the occurrence of a knock with high ammonia substitution can be decreased, and the unburned fuel emission during valve overlap can be lowered when ammonia is directly injected [9]. In addition, the phenomenon of ammonia occupying the volume of fresh air can be eliminated by ammonia direct injection.

Note that liquid ammonia is highly susceptible to flash boiling at engine-like conditions due to the low boiling point. Thus, the characteristics of ammonia spray and air-fuel mixture formation are different from traditional hydrocarbon fuel. In spite of this, flash boiling spray of ammonia is considered to be a promising fuel injection method. In internal combustion engine engineering, flash boiling spray can greatly improve spray characteristics such as initial spray cone angle, initial Sauter mean diameter (SMD), spray evaporation rate, spray penetration, and the width of the fully developed spray dense area, thus improving the fuel and air mixing process. Scharl et al. [4] found that ammonia combustion is sensitive to the interaction between ammonia direct injection and charge condition. Additionally, due to the low boiling point, liquid ammonia is highly susceptible to flash boiling even at high pressure and temperatures. Li et al. [5] investigated the near- and far-field characteristics of superheated ammonia spray. They found that both superheat degree and fuel viscosity play a significant role in the entire flashing region. Pelé et al. [10] conducted a comparative study on the spray characteristics of ammonia, biofuel, ethanol, and gasoline with a current spark ignition GDI (Gasoline direct injection) injector. They found that the jet structure of ammonia greatly differs from that of other fuels. Additionally, the flash boiling condition at ambient temperature was explored for ammonia and indicated a wider spray at half-penetration length at phase change. Liu et al. used open Foam to conduct a fluid simulation of low-temperature nitrogen and non-low-temperature n-dodecane and ammonia spray under supercritical conditions and found that n-dodecane has higher density and viscosity under supercritical conditions, resulting in higher jet velocity and higher spray concentration [8]. Recently, Tang et al. [11] investigated the spray macroscopic and microscopic characteristics at non-flash, transition flash, and flare flash boiling regions with a single-hole injector. They found that the spray significantly expands in the radial direction at flare flash boiling regions ($R_p \leq 0.47$, R_p is the ratio of the ambient pressure P_{amb} and the saturated vapor pressure P_{sat} at the liquid temperature), while the spray contracts in the penetration direction at the transition flash boiling region ($0.47 < R_p \leq 1.06$). In addition, the macroscopic spray of liquid ammonia demonstrated that the higher the R_p, the larger the droplet size number, resulting in more uniformly distributed droplet sizes and an increased Sauter mean diameter.

For port fuel injection, there is no need to increase the injection pressure when gaseous ammonia is used due to the low boiling point. However, for direct injection, increasing the injection pressure is regarded as an effective approach in improving the combustion and emissions of ammonia engines, especially for dual fuel dual injection engines. Although there are some studies focusing on liquid ammonia injection relating to flash boiling, the injection pressures are less than 30 MPa. Therefore, there is a research gap related to liquid ammonia direct injection under high pressure at different boiling flash regions.

In this study, a single-hole injector was used to analyze the characteristics of liquid ammonia spray to avoid plumes of multi-hole interactions. The spray characteristics of liquid ammonia under various ambient pressures and temperatures were analyzed in a constant volume chamber to cover a wide range of superheat degrees. This study provides sufficient data related to flash boiling ammonia sprays and critical information for understanding the mechanism and developing simulation models of flash boiling ammonia sprays.

2. Experimental Setup and Procedure

2.1. Experimental Setup

The main experimental device of the constant volume vessel used in the experiment is composed of stainless-steel outside, high temperature ceramic furnace inside, high pressure manual oil pump, fuel tank, filter and electronic controller, as shown in Figure 1.

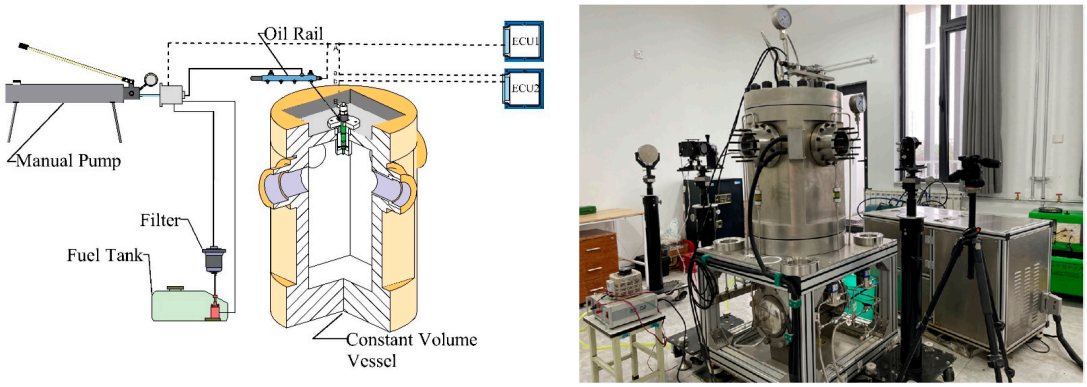

Figure 1. Schematic of the experimental apparatus.

A high-pressure common rail fuel injector is installed on the top of the constant volume vessel, and a cylindrical vessel formed by the hollow part of the bomb is used to simulate the high-temperature and high-pressure environment of the combustion chamber of the internal combustion engine. There are four cylindrical windows on the side wall of the bomb to study the spray and combustion characteristics of the fuel (such as diesel and gasoline). The system can provide injection pressures ranging from 60 to 120 MPa, which meets the injection pressure requirement of 70 MPa and 80 MPa in this experiment.

In the liquid ammonia spray experiment, the images of the gas and liquid phases were collected using the Schlieren method [12]. This method [13] adopts a typical "Z-shaped" optical path diagram in which the halogen lamp becomes the light source, the main and secondary mirrors are two spherical mirrors, and the rectangular area in the middle is the fluid acquisition area, which is collected by a high-speed camera. In the experiment, the light sent out by the halogen light source is reflected by the reflector through the fluid acquisition area. Afterward, it will be reflected by another emitter mirror, cut in half of the knife edge, which is perpendicular to the density gradient of the flow field, and finally delivered into the imaging system (high-speed camera). The fluid will be collected with different flow densities [12]. The product model of the high-speed camera is Photron Fastcam mini AX200 with an AF-S VR Micro-Nikkor 105 mm f/2.8G IF-ED Lens. The preservation of the collected images of spray development is transmitted through Photron's

Fastcam Viewer 4.0, which uses a high-speed internet interface to connect to the high-speed camera and save the images to the computer promptly. The measurement technique is mainly collected by a high-speed camera; the minimum shutter speed of the camera can be set is 1.05 us; and the frame rate is 20,000 fps. For the data acquisition system, the wiring harness connection includes a power supply box, heating cable, thermocouple, temperature and pressure sensor, inlet and exhaust, solenoid valve, etc. The data acquisition control system can adjust the ambient temperature inside the tank by controlling the opening of the power regulator and change the ambient pressure inside the tank by controlling the opening and closing of the inlet and exhaust solenoid valves. The speed of the oil supply system pump can be adjusted by the frequency converter, and the PID controller can adjust or keep the rail pressure stable.

2.2. Test Conditions and Procedure

In this experiment, liquid ammonia was used as the fuel, and the ambient gas in the bomb was nitrogen due to its inertia. Nitrogen, a colorless and odorless gas at normal temperatures, is difficult to react with other substances, and its chemical properties are relatively stable and widely obtained. The experimental conditions and key parameters are shown in Table 1. During the experiment, the ambient temperature in the tank was preheated to 500 K, while the temperature of liquid ammonia fuel was adjusted to 320 K. The diameter of the spray hole at the top of the bomb tolerance is 0.14 mm, and the injection duration is set to 1.0 ms, which is the same under all working conditions.

Table 1. Key parameters of experimental conditions.

Items	Parameters
Ambient temperature (T_{amb}, K)	500
Ambient pressure (P_{amb}, MPa)	0.2, 0.6, 2, 3, 4
Injection pressure (P_{inj}, MPa)	70, 80
Fuel	Liquid ammonia
Fuel temperature (T_f, K)	320
Spray hole diameter (mm)	0.14
Fuel saturated vapor pressure (MPa)	1.87
Injection duration (ms)	1.0

The experimental conditions, including the ambient pressure (P_{amb}) and injection pressure (P_{inj}), are listed in Table 2. On the basis of the definition of superheat degree (ratio of ambient pressure P_{amb} to saturated vapor pressure P_{sat} at the liquid temperature) [5], the saturated vapor pressure of liquid ammonia at 320 K is near 1.87 MPa (as can be shown in Table 1). All these experimental cases cover non-flash boiling spray ($R_p > 1.0$), transition flash boiling spray ($0.3 < R_p < 1.0$), and flare flash boiling spray ($R_p < 0.3$). The shape of the ammonia spray under three boiling states is shown in Figure 2. Meanwhile, we used two different injection pressures under each environmental pressure condition to ensure the accuracy and generality of the experiment and the high injection pressure of the spray.

Table 2. Experimental cases.

Cases	P_{amb} (MPa)	P_{amb} (MPa)	Ambient Gas	Spray State	R_p
1 2	0.2	70 80	N_2	Flare flash boiling	0.11
3 4	0.6	70 80	N_2	Transition flash boiling	0.32
5 6	2	70 80	N_2	Non-flash boiling	1.07
7 8	3	70 80	N_2	Non-flash boiling	1.60
9 10	4	70 80	N_2	Non-flash boiling	2.14

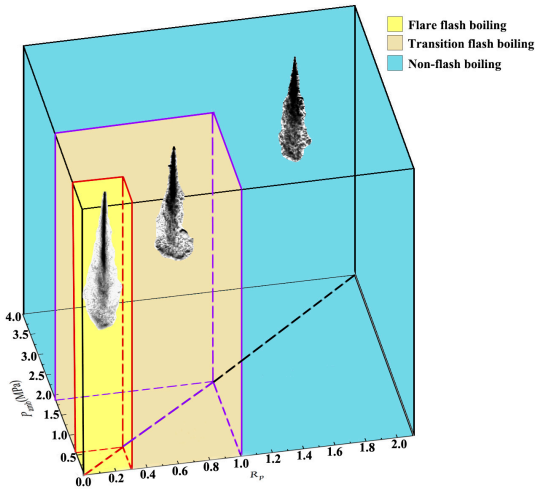

Figure 2. Relationship between cylinder pressure and superheat at 320 K fuel temperature.

3. Results and Discussion

According to the meaning of superheat degree [5], when the ambient pressure is 0.2 MPa, the superheat degree (R_p) of liquid ammonia is less than 0.3 [14]. When the ambient pressure is 0.6 MPa, the liquid ammonia spray is in a transition flash boiling state, and the Rp of liquid ammonia is between 0.3 and 1.0. When the ambient pressure is 2.0, 3.0, and 4.0 MPa [11], the R_p of liquid ammonia is beyond 1, and the liquid ammonia spray is non-flash boiling spray under these ambient pressures. Therefore, the following section will explore the influence of injection and ambient pressures during the development of liquid ammonia spray, particularly flash boiling spray.

3.1. Effect of Injection Pressure of Ammonia on Spray

3.1.1. Non-Flash Boiling Spray

We set the ambient pressure as 2.0 MPa according to Table 3 and superheated degree to control the liquid ammonia spray into the state of non-flash boiling. As shown in Table 4, the morphologic changes in non-flash boiling spray with time under two injection pressures can be observed. As the injection pressure increases, it is apparent that the spray speed of liquid ammonia is accelerated; thus, the development of non-flash boiling spray is also accelerated.

Table 3. Spray state division.

Superheat Range	Spray Type
$R_p < 0.3$	Flare flash boiling
$0.3 < R_p < 1.0$	Transition flash boiling
$1.0 < R_p$	Non-flash boiling spray

The development of gas–liquid penetration under different injection pressures is revealed in Figure 3. Two different injection pressures (70 and 80 MPa) are set. From this figure, it is obvious that with the enlargement of injection pressure, both the liquid and gas penetration of ammonia rose. It is obvious that this result is roughly the same as the result and trend of his article on ammonia spray under different injection pressures [15]. In addition, the law of development of liquid penetration is more complicated than that of gas penetration. First, for liquid penetration, one of the most apparent characteristics is that penetration will fluctuate in the later stage of spray development. An important factor that causes the fluctuation of liquid penetration is that the high in-cylinder temperature (500 K) may lead to fluctuations in the cylinder pressure, and it will exert a force on the oil droplets in the liquid phases.

Table 4. Development of non-flash boiling spray over time.

Fuel	0.0 ms	0.1 ms	0.2 ms	0.3 ms	0.4 ms	0.5 ms	0.6 ms
Ammonia (70 MPa)	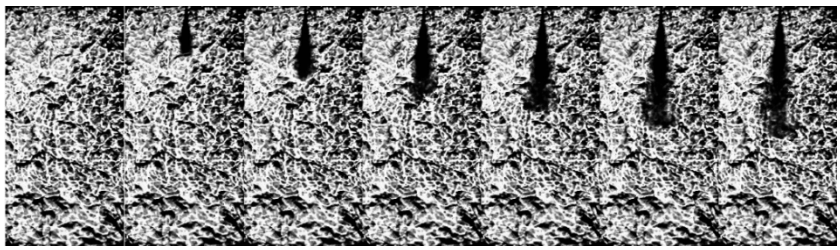						
Ammonia (80 MPa)	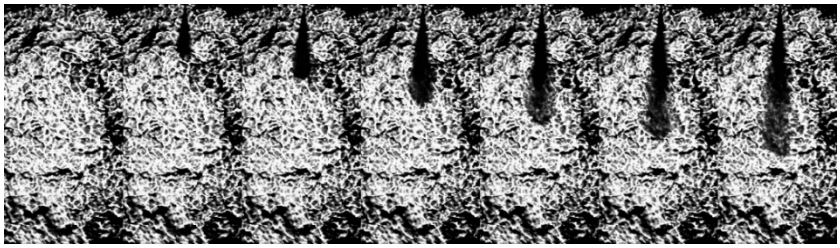						

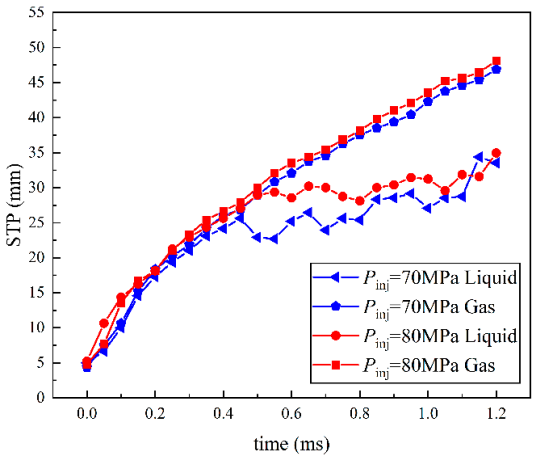

Figure 3. Non-flash boiling spray penetration distance development (P_{amb} = 2.0 MPa).

Another significant feature that can be captured in Figure 3 is that the spray tip penetration (STP) of the gas–liquid phase of the spray will separate gradually over time, and gas penetration will slowly increase while the liquid penetration length will stabilize after fluctuations and no longer change [16]. The reason for this phenomenon is that the liquid ammonia spray gradually vaporizes under the high temperature environment in the tank, and the liquid phase region decreases while the gas phase region increases. Compared to liquid penetration, the gas penetration under these injection pressures is smoother, and gas penetration keeps growing. This is because ammonia droplets will break and evaporate into gas molecules under the high pressure inside the nozzle and high temperature of the fuel.

The development of the gas–liquid area under different injection pressures is shown in Figure 4. In general, the overall change trend of the gas–liquid spray area is consistent with the penetration. With the variation in the injection pressure from 70 to 80 MPa, liquid and gas spray areas both become larger. At the same time, as injection pressure increased, the separation time of the gas–liquid region was advanced because the pressure difference between the inside and outside of the spray hole was increased. Therefore, the fragmentation and atomization of liquid fuel is enhanced, speeding up the vaporization of small droplets. Additionally, the change law of spray area and the development law of spray penetration distance corroborate each other's variation, proving the accuracy and rigor of the whole experiment.

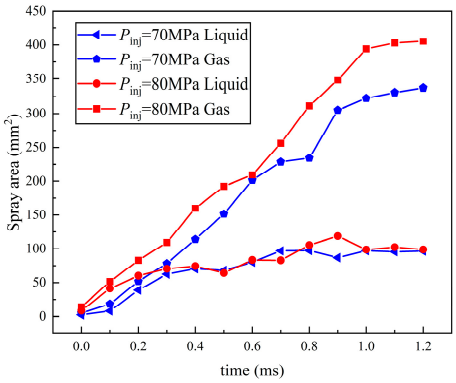

Figure 4. Non-flash boiling spray area development (P_{amb} = 2.0 MPa).

3.1.2. Transition Flash Boiling Spray

In this section, we set the ambient pressure as 0.6 MPa according to Table 3 and the definition of superheat degree to control the liquid ammonia spray form into transition flash boiling spray. For this state of spray, two injection pressures, 70 and 80 MPa, are also set to confirm the law of its development. Five different injection pressures have a certain influence on the penetration of transition flash boiling spray, as depicted in Table 5.

Table 5. Development of transition flash boiling spray over time.

Fuel	0.0 ms	0.1 ms	0.2 ms	0.3 ms	0.4 ms	0.5 ms	0.6 ms
Ammonia (70 MPa)	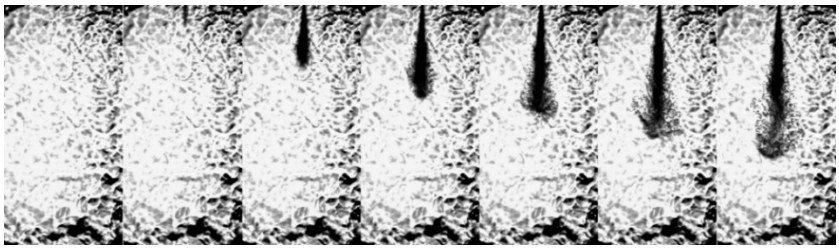						
Ammonia (80 MPa)	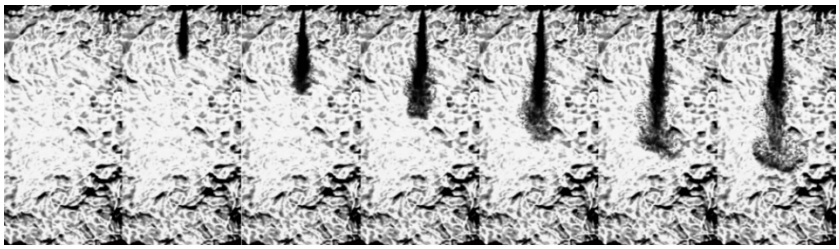						

The effect of injection pressure on the development of transitional flash boiling spray is similar to that of non-flash boiling spray. As the injection pressure increases, the injection of transitional flash boiling spray is accelerated, the fuel vaporization at the front end of the spray is enhanced, and the gas diffusion is also enhanced after 0.6 ms.

Based on Figure 5, the effect of injection pressure on the transition flash boiling spray is simple and clear (i.e., the gas penetration of liquid ammonia transition flash boiling spray will be increased with the increase in injection pressure). When the injection pressure increases from 70 to 80 MPa, the fuel droplets obtain more kinetic energy from the spray hole, and they can move and propel farther. As for the liquid phase penetration distance, based on Figure 5, it increases with the increase in injection pressure at the initial stage of spraying, while the vaporization is accelerated under the influence of the flash boiling phenomenon that occurs at the later stage of spraying. Therefore, the liquid penetration length under both injection pressures tends to become flat in the later stages of development, and the gap between gas and liquid penetration is not large. Due to the increased vaporization and boiling of transitional flash boiling spray, the variation in

injection pressure has a more apparent influence on the vapor penetration length, and the gas penetration increases as injection pressure increases, just like liquid penetration.

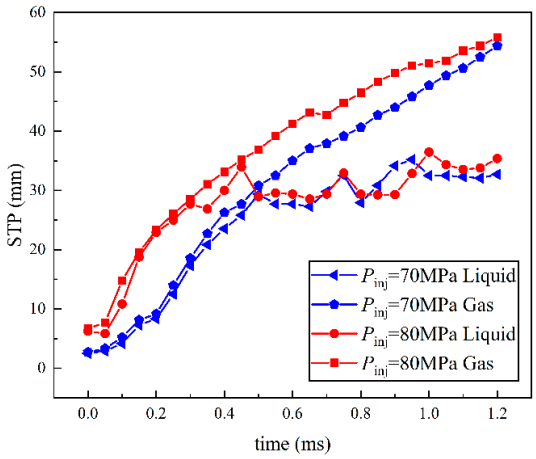

Figure 5. Development of transition flash boiling spray penetration over time (P_{amb} = 0.6 MPa).

Figure 6 shows the development of transition flash boiling spray areas. With the increase in the injection pressure, the spray area grew simultaneously. By comparing Figures 5 and 6, the effect of injection pressure on transition flash boiling spray is approximately the same as that of the non-flash boiling spray. As the injection pressure increased, the growth degree of the gas spray area is much more apparent than that of the liquid spray area, for similar reasons to the above influence on the penetration distance.

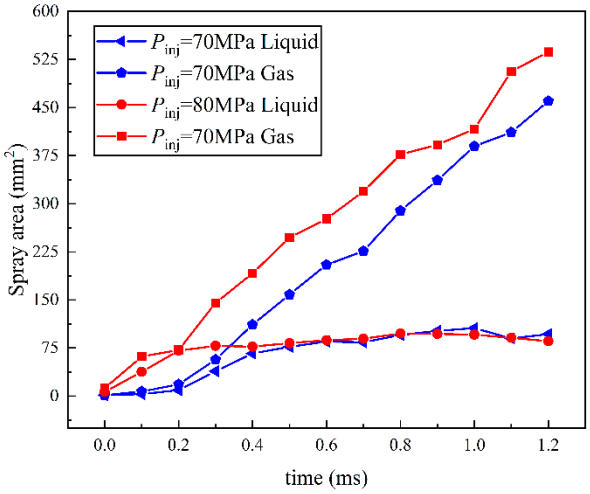

Figure 6. Development of transition flash boiling spray area over time (P_{amb} = 0.6 MPa).

3.1.3. Flash Boiling Spray

In this section, we set the ambient pressure as 0.2 MPa according to Table 3 and the related chart of superheat degree to adjust the liquid ammonia spray into flare flash boiling spray [17].

Table 6 shows the morphometric development of flare flash boiling spray with time under two injection pressures at a back pressure of 0.2 MPa. Similar to the properties and characteristics of non-flash boiling spray and transition flash boiling spray, the development of flare flash-boil spray has a tendency to accelerate with the increased injection pressure [18]. The STP between the gas and liquid phases of flash boiling spray is stretched. However, compared to non- and transition-flash boiling sprays, the later development of spray in the graph in which the spray cone angle of flash boiling spray is significantly

reduced [11]. In addition, the spray cone angle of the flash boiling spray also decreases with the variation in injection pressure from 70 to 80 MPa. When the injection pressure is 80 MPa, the shape of flash boiling spray is very close to that of a needle, and the vaporization at the front end of the spray region is accelerated.

Table 6. Development of flash boiling spray over time (P_{amb} = 0.2 MPa).

Fuel	0.0 mms	0.1 ms	0.2 ms	0.3 ms	0.4 ms	0.5 ms	0.6 ms
Ammonia (70 MPa)	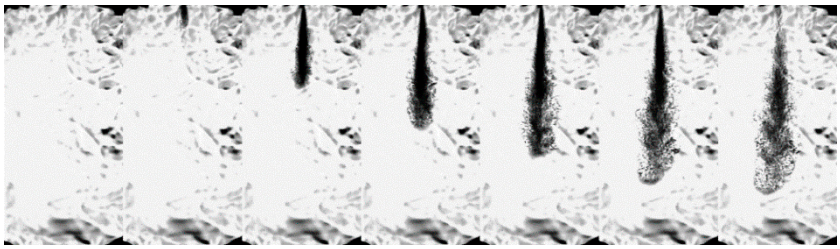						
Ammonia (80 MPa)	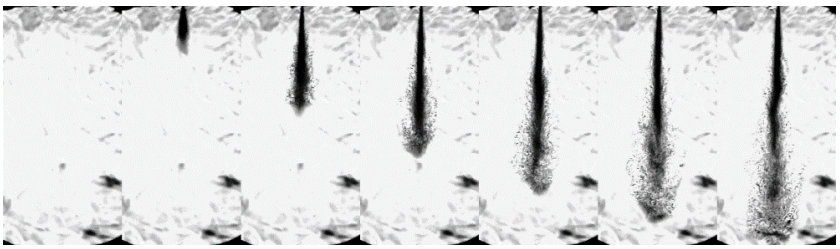						

As shown in Figure 7, the penetration distance of flash boiling spray increases with the elevation of the injection pressure, which is much the same as that of non-flash and transition-flash boiling sprays. More of that, compared with the first two spray states, the liquid phase penetration distance of flare flash boiling spray fluctuates more intensively in the later stage. This can be attributed to the increase in the injection pressure and flare flash boiling phenomenon that strengthens the interaction between the fuel droplets and the ambient gas inside the cylinder, and the interaction between them accelerates the breakup and evaporation of the droplets, resulting in a larger spray penetration gap, which is similar to the discovery of Zhang et al. [19]. Another factor causing this phenomenon can be the high temperature in the bomb, which is 500 K. The high temperature will also accelerate the vaporization rate of fuel droplets so that the process of droplets transforming into gas molecules will be accelerated [16]. Figure 8 shows that, with the increase in injection pressure, the gas spray area increases to a greater extent than the liquid area. The gas area of the spray has an obvious growth trend and an increase in the later stage that the fragmentation and atomization of the fuel bubbles of ammonia become expedited due to the phenomenon of the flare flash boiling [20].

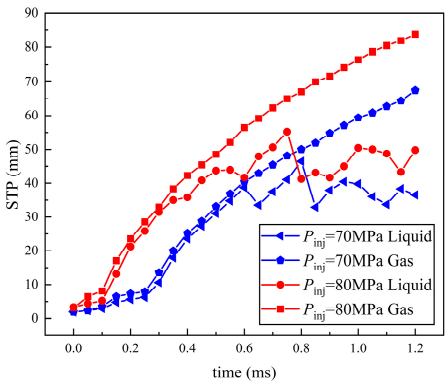

Figure 7. Development of flash boiling spray penetration over time (P_{amb} = 0.2 MPa).

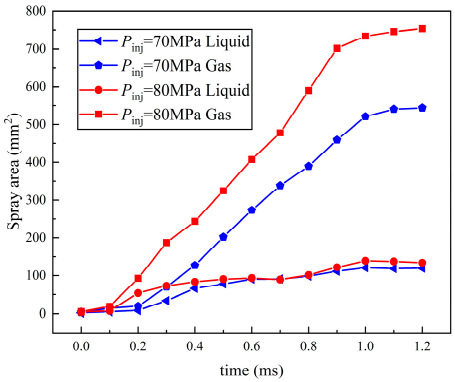

Figure 8. Development of flash boiling spray area over time (P_{amb} = 0.2 MPa).

3.2. Influence of Ambient Pressure on Liquid Ammonia Spray and the Appearance of Spray Resistance Phenomenon

3.2.1. Influence of Ambient Pressure on Three Kinds of Spray under 70 MPa Injection Pressure

In this study, the data of liquid ammonia spray in different states under three different ambient pressures were compared to explore the differences between the flare flash boiling spray and the other two kinds of spray. The ambient pressure at the state of non-flash boiling spray is 2.0 MPa, for transient flash boiling spray is 0.6 MPa, and for flare flash boiling spray is 0.2 MPa. The penetration and spray area development of the three sprays were compared, as shown in Figures 9 and 10. In the figure below, the injection pressure of liquid ammonia spray is 70 MPa.

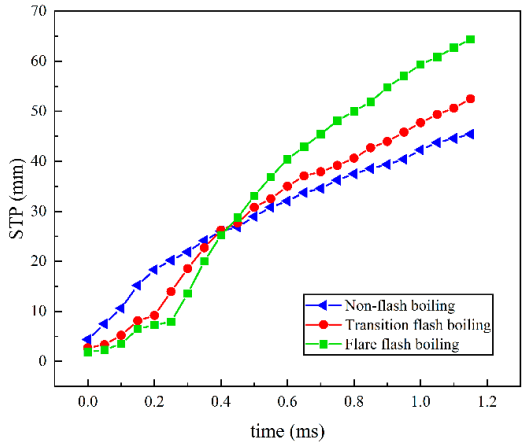

Figure 9. Comparison of gas penetration distance of spray in three states (P_{inj} = 70 MPa).

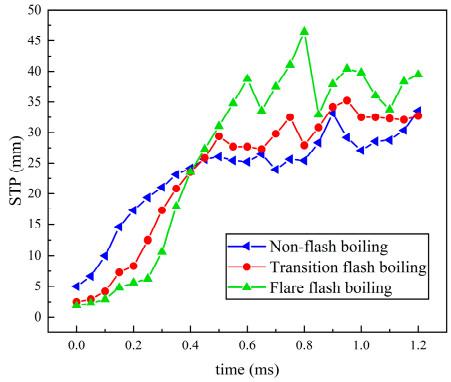

Figure 10. Comparison of liquid penetration length of spray in three states (P_{inj} = 70 MPa).

In Figures 9 and 10, based on the comparison of gas and liquid penetration, the developing trend is roughly the same, despite that the liquid penetration fluctuates in different extents after above 0.4 ms of the injection, and does not significantly increase any more after the fluctuation. In the analysis, we set the spray to 0.4 ms as the node of the progress. Between the start of spray and 0.4 ms, the penetration distance of non-flash boiling spray grew faster than that of transient flash boiling spray, while the developments' speed of penetration of flare flash boiling spray is the slowest [21]. Before 0.4 ms, the penetration distance of the three sprays was the same at a certain time point. After 0.4 ms, the STP of flare flash boiling spray significantly accelerated, and the growth rate was faster than that of other two kinds of sprays. Due to the low back pressure of flash boiling state, the STP of the fuel is abnormally shortened at a very low environmental density inside the vessel, which is named as "spray resistance phenomenon" [21]. In Section 3.2.2, this phenomenon will be discussed further.

3.2.2. Effect of Ambient Pressure on Spray under 80 MPa Injection Pressure

In contrast with Section 3.2.1, the phenomenon of spray resistance under the injection pressure of 80 MPa arises earlier than that under the pressure of 70 MPa. Under this circumstance, four more conditions of ambient pressures were added under the premise that the spray pressure of 80 MPa, and the ambient pressures of 0.2, 2, 3, and 4 MPa. Furthermore, despite the fact that the spray is under the ambient pressure of 0.2 MPa, which is in a flare flash boiling state, the sprays are at cold conditions. Thus, the relevant characteristics of flash boiling spray can be analyzed.

Table 7 illustrates the development characteristics of the ammonia spray under different ambient pressures in the early spray stage. At 0.1 ms, the form of flash boiling spray at 0.2 MPa is smaller than that of cold (non-flash boiling) spray at the other three ambient pressures. After 0.2 ms, the flash boiling spray has rapidly developed and obviously exceeds the other three non-flash boiling sprays. These results also illustrated the spray resistance phenomenon in the comparison of three different spray states in the previous section. Subsequently, this phenomenon will be further understood and explained by exploring and comparing the STP and spray area under four different ambient pressures.

In Figure 11, the gas penetration is shown on the graph. In Figure 11, which illustrates the development of gas STP under different ambient pressures. For the injection pressure of 80 MPa, flash boiling was confirmed to happening when P_{amb} (ambient pressure) is 0.2 MPa, and the other Pamb makes it as the cold conditions. Furthermore, after the injection pressure is lifted up to 80 MPa, the spray resistance of the STP is advanced from 0.4 to 0.15 ms.

Moreover, in the flare flash boiling state, the development of STP from the beginning of spray at 0.2 ms was relatively slow in the early stage but developed rapidly in the later stage. The trend in P_{amb} = 0.2 MPa is distinguished from that in P_{amb} = 2–4 MPa. At approximately 0–0.15 ms in the initial stage of spray process, the gas STP under flare flash boiling conditions were lower than that under cold conditions, although the ambient density under flare flash boiling conditions was lower than those under the non-flash boiling conditions. This is because, at P_{amb} of 0.2 MPa, liquid ammonia which is filled with the spray hole generates intensive cavitation at the time when injector needle started lifting [21–23], this behavior will block the nozzle and cause a different tendency with a shorter penetration than the other cold conditions in the initial stage. Additionally, similar results were also found in the research of Ainsalo [24], although he investigated high-pressure propane sprays using a diesel injector.

In Figure 12, where spray gas areas are analyzed, the area variation trend in P_{amb} of 0.2 MPa was observed to be different from others. This is because the P_{amb} of 0.2 MPa created flash boiling conditions. The gas areas are shown on the graph.

Table 7. Development of ammonia spray under different ambient pressures (P_{inj} = 80 MPa).

Fuel	0.0 ms	0.1 ms	0.2 ms	0.3 ms	0.4 ms
P_{amb} = 0.2 MPa	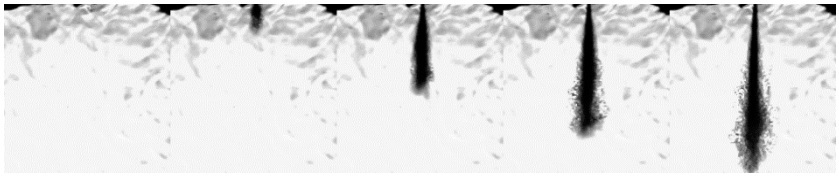				
P_{amb} = 2.0 MPa	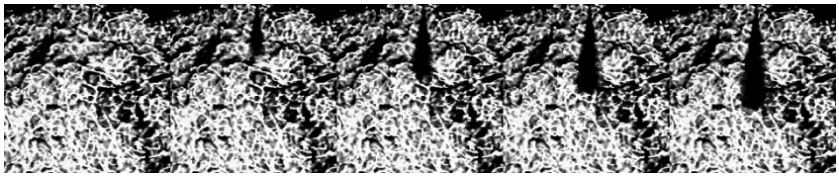				
P_{amb} = 3.0 MPa	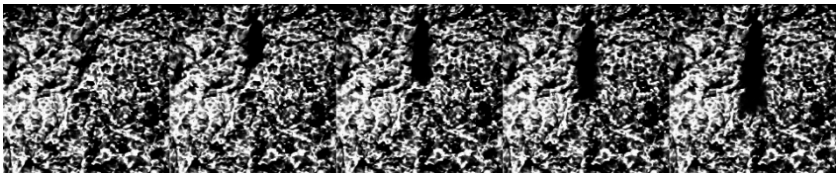				
P_{amb} = 4.0 MPa	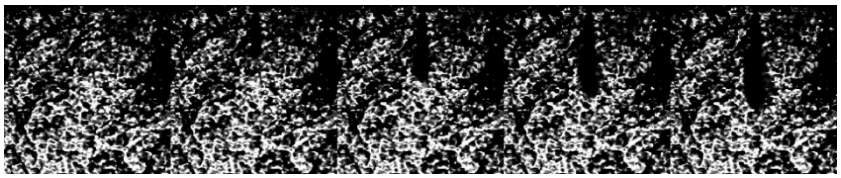				

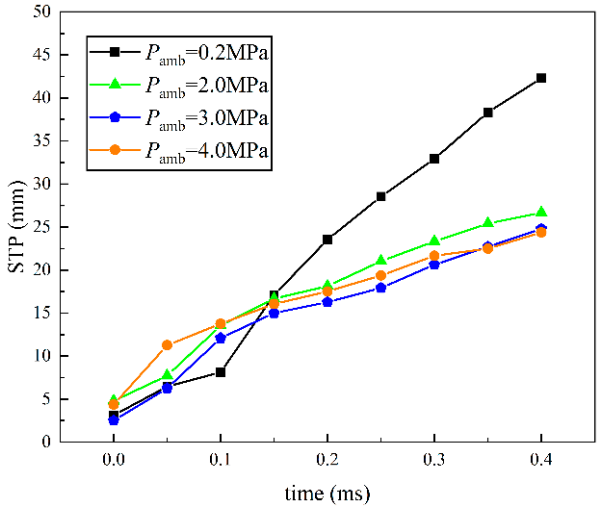

Figure 11. Development of spray gas penetration under different ambient pressures (P_{inj} = 80 MPa).

The comparison results of gas spray area are similar to the gas STP. Moreover, after the phenomenon of spray resistance appears, the spray developed faster as the ambient pressure decreased. The enlarging ambient pressure will slow the spray development and have impacts on the spray area and STP. It is due to the pressure discrepancy inside and outside the spray hole narrowed as the ambient pressure increased. Fuel is affected by environmental stress, movement is hindered and the greater the pressure, the greater the restriction of fuel development.

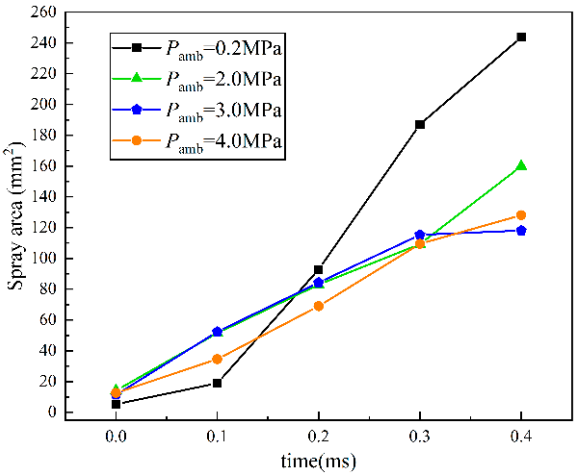

Figure 12. Development of spray gas areas under different ambient pressures (P_{inj} = 80 MPa).

4. Conclusions

In this study, the influence of spray pressure on the non-flash, transition flash and flare flash boiling sprays was explored by comparing the spray experiment in the capacity of the projectile and the relevant characteristics of the three types of spray. Ultimately, the spray development under different ambient pressures was further explored.

1. The gas–liquid STP of cold spray was not significantly changed by the injection pressure, although the STP was increased to some extent. For flash boiling spray, including transition and flare flash boiling sprays, the STP of the gas and liquid increased more than that of cold spray, and the fluctuation of the late spray was relatively large. Therefore, the injection pressure has a greater effect on the penetration distance of flash boiling spray.
2. The variation trend of spray area was consistent with the STP, confirming the accuracy of the experiment. Under the influence of injection pressure, the separation time of the spray area is earlier than that of gas–liquid STP. The liquid spray area of the three kinds of spray is not affected by the injection pressure, and the final area of the liquid phase region is similar to that of the development of spray. The growth of the gas area is greatly affected by the injection pressure. Meanwhile, the gas area of flare and transition flash boiling spray is much larger than that of cold spray, and the growth degree of flash boiling spray is greater than that of cold spray.
3. The spray resistance phenomenon was confirmed by comparing the STP of spray under three states with that under different ambient pressures. Under the spray pressure of 70 MPa, the spray appears at the inter section point of approximately 0.4 ms, and the spray resistance phenomenon appears before 0.4 ms. The ambient pressure of flash boiling spray is much smaller than that of cold spray. At a low environmental density, the STP of spray is abnormally shortened. Spray resistance increased to approximately 0.15 ms as the injection pressure increased. Since the ambient pressure of flash boiling spray was only 0.2 MPa, which was much lower than that under the other three kinds of cold spray, the spray resistance also occurred.

Author Contributions: Methodology, L.W.; Investigation, H.H.; Resources, H.L.; Writing—original draft, L.H.; Writing—review & editing, Z.C.; Supervision, S.L.; Funding acquisition, H.H., J.W., L.W. and H.L. All authors have read and agreed to the published version of the manuscript.

Funding: This project was funded by Natural Science Foundation of the Zhejiang Province (Grant No. LQ22E060001), China Postdoctoral Science Foundation (2023M741840), Shaanxi Science and technology Nova (2024ZC-KJXX-026), Young Innovative Talent Program (Grant No. 2022A-135-G), and Ningbo Major Research and Development Plan Project (Grant No. 2022Z151).

Data Availability Statement: The original contributions presented in the study are included in the article, further inquiries can be directed to the corresponding author.

Acknowledgments: Our deepest gratitude goes to the editors and reviewers for their careful work and thoughtful suggestions, which have helped us to improve this paper substantially.

Conflicts of Interest: Authors Haibin He, Jie Wu, Lei Wang, Hua Lou, Songfeng Li and Zhanming Chen were employed by the company Ningbo C.S.I. Power & Machinery Group Co., Ltd. The remaining authors declare that the research was conducted in the absence of any commercial or financial relationships that could be construed as a potential conflict of interest.

References

1. Pham, Q.; Park, S.; Agarwal, A.K.; Park, S. Review of dual-fuel combustion in the compression-ignition engine: Spray, combustion, and emission. *Energy* **2022**, *250*, 123778. [CrossRef]
2. Yang, W.; Ranga Dinesh, K.K.J.; Luo, K.H.; Thevenin, D. Direct numerical simulation of turbulent premixed ammonia and ammonia-hydrogen combustion under engine-relevant conditions. *Int. J. Hydrogen Energy* **2022**, *47*, 11083–11100. [CrossRef]
3. Liu, Z.; Zhou, L.; Zhong, L.; Wei, H. Enhanced combustion of ammonia engine based on novel air-assisted pre-chamber turbulent jet ignition. *Energy Convers. Manag.* **2023**, *276*, 116526. [CrossRef]
4. Scharl, V.; Lackovic, T.; Sattelmayer, T. Characterization of ammonia spray combustion and mixture formation under high-pressure, direct injection conditions. *Fuel* **2023**, *333*, 126454. [CrossRef]
5. Li, S.; Li, T.; Wang, N.; Zhou, X.; Chen, R.; Yi, P. An investigation on near-field and far-field characteristics of superheated ammonia spray. *Fuel* **2022**, *324*, 124683. [CrossRef]
6. Wang, N.; Huang, S.; Zhang, Z.; Li, T.; Yi, P.; Wu, D.; Chen, G. Laminar burning characteristics of ammonia/hydrogen/air mixtures with laser ignition. *Int. J. Hydrogen Energy* **2021**, *46*, 31879–31893. [CrossRef]
7. Dimitriou, P.; Javaid, R. A review of ammonia as a compression ignition engine fuel. *Int. J. Hydrogen Energy* **2020**, *45*, 7098–7118. [CrossRef]
8. Liu, X.; Tang, Q.; Im, H.G. Enhancing ammonia engine efficiency through pre-chamber combustion and dual-fuel compression ignition techniques. *J. Clean. Prod.* **2024**, *436*, 140622. [CrossRef]
9. Zhang, Z.; Long, W.; Dong, P.; Tian, H.; Tian, J.; Li, B.; Wang, Y. Performance characteristics of a two-stroke low speed engine applying ammonia/diesel dual direct injection strategy. *Fuel* **2023**, *332*, 126086. [CrossRef]
10. Pelé, R.; Mounaïm-Rousselle, C.; Bréquigny, P.; Hespel, C.; Bellettre, J. First Study on Ammonia Spray Characteristics with a Current GDI Engine Injector. *Fuels* **2021**, *3*, 253–271. [CrossRef]
11. Liu, X.; Yao, X.; Wang, Z.; Tang, C. Single hole ammonia spray macroscopic and microscopic characteristics at flare and transition flash boiling regions. *Appl. Therm. Eng.* **2023**, *235*, 121443. [CrossRef]
12. Settles, G.S. Schlieren and Shadowgraph Techniques: Visualizing Phenomena in Transport Media. *Appl. Mech. Rev.* **2002**, *55*, B76. [CrossRef]
13. Gladstone, J.H.; Dale, T.P. Researches on the Refraction, Dispersion, and Sensitiveness of Liquids. *Philos. Trans. R. Soc. Lond.* **1863**, *153*, 317–343.
14. Lewandowski, M.T.; Pasternak, M.; Haugsvær, M.; Løvås, T. Simulations of ammonia spray evaporation, cooling, mixture formation and combustion in a direct injection compression ignition engine. *Int. J. Hydrogen Energy* **2023**, *52*, 916–935. [CrossRef]
15. Huang, Z.; Wang, H.; Luo, K.; Fan, J. Large eddy simulation investigation of ammonia spray characteristics under flash and non-flash boiling conditions. *Appl. Energy Combust. Sci.* **2023**, *16*, 100220. [CrossRef]
16. An, Z.; Xing, J.; Kurose, R. Numerical study on the phase change and spray characteristics of liquid ammonia flash spray. *Fuel* **2023**, *345*, 128229. [CrossRef]
17. Xu, M.; Zhang, Y.; Zeng, W.; Zhang, G.; Zhang, M. Flash Boiling: Easy and Better Way to Generate Ideal Sprays than the High Injection Pressure. *SAE Int. J. Fuels Lubr.* **2013**, *6*, 137–148. [CrossRef]
18. Zhang, Z.; Li, T.; Chen, R.; Wang, N.; Wei, Y.; Wu, D. Injection characteristics and fuel-air mixing process of ammonia jets in a constant volume vessel. *Fuel* **2021**, *304*, 121408. [CrossRef]
19. Zhang, Y.; Xu, L.; Zhu, Y.; Xu, S.; Bai, X.-S. Numerical study on liquid ammonia direct injection spray characteristics under engine-relevant conditions. *Appl. Energy* **2023**, *334*, 120680. [CrossRef]
20. Gao, S.; Yan, J.; Lee, T.H.; Lee, C.-F. Model development for flash boiling spray and validations with isooctane, hexane, ethanol and their binary mixtures. *Fuel* **2022**, *321*, 123917. [CrossRef]
21. Fang, Y.; Ma, X.; Zhang, Y.; Li, Y.; Zhang, K.; Jiang, C.; Wang, Z.; Shuai, S. Experimental Investigation of High-Pressure Liquid Ammonia Injection under Non-Flash Boiling and Flash Boiling Conditions. *Energies* **2023**, *16*, 2843. [CrossRef]
22. Liu, X.; Zaihi, A.; Al-lehaibi, M.; Mohan, B.; AlRamadan, A.; Cenker, E.; Im, H.G. Investigation of the Cryogenic Nitrogen and Non-Cryogenic N-Dodecane and Ammonia Injections using a Real-Fluid Modelling Approach. *SAE Int. J. Adv. Curr. Pract. Mobil.* **2022**, *5*, 1129–1141. [CrossRef]

23. Liu, X.; Guo, J.; Im, H.G. Development of correlation model for cavitating spray using Eulerian simulations. *Int. J. Engine Res.* **2023**, *25*, 613–630. [CrossRef]
24. Ainsalo, A.; Sallinen, R.; Kaario, O.; Larmi, M. Optical investigation of spray characteristics for light fuel oil, kerosene, hexane, methanol, and propane. *At. Sprays* **2019**, *29*, 521–544. [CrossRef]

Disclaimer/Publisher's Note: The statements, opinions and data contained in all publications are solely those of the individual author(s) and contributor(s) and not of MDPI and/or the editor(s). MDPI and/or the editor(s) disclaim responsibility for any injury to people or property resulting from any ideas, methods, instructions or products referred to in the content.